Solving the discrepancy among the light elements abundances and WMAP

Kazuhide Ichikawa,* Masahiro Kawasaki, and Fuminobu Takahashi

Institute for Cosmic Ray Research, University of Tokyo,
5-1-5 Kashiwa-no-Ha, Kashiwa City, Chiba 277-8582, Japan
(Dated: February 2, 2008)

Within the standard big bang nucleosynthesis (BBN) and cosmic microwave background (CMB) framework, the baryon density measured by the Wilkinson Microwave Anisotropy Probe (WMAP) or the primordial D abundance is much higher than the one measured by the ^{4}He or ^{7}Li abundances. To solve the discrepancy, we propose a scenario in which additional baryons appear after BBN. We show that simply adding the baryons can not be a solution but the existence of a large lepton asymmetry before BBN makes the scenario successful. These extra baryons and leptons, in addition to the initial baryons which exist before the BBN, can be all produced from Q-balls.

I. INTRODUCTION

The baryon density is one of the most important cosmological parameters. Especially, it is the only one input parameter for the standard big bang nucleosynthesis (BBN) theory, which predicts the abundances of light elements, D, ^{4}He and ^{7}Li. Meanwhile, for the cosmic microwave background (CMB), it also plays an important role in determining the shape of the acoustic peaks. Observations of the three light elements and the CMB on the whole indicate equal amount of baryons and make us confirm the validity of the standard cosmology.

Recently, following the precise measurement of the CMB by the Wilkinson Microwave Anisotropy Probe (WMAP), its concordance with the BBN and the light elements observations has been investigated in Refs [1, 2, 3, 4]. The baryon density measured from the WMAP data is $\omega_b \equiv \Omega_b h^2 = 0.024 \pm 0.001$ (with the power-law ΛCDM model) [5], where Ω_b is the baryon energy density divided by the critical energy density today and h is the Hubble constant in units of 100 km s^{-1} Mpc^{-1}. The uncertainty is very small because the WMAP has detected the first and second peaks accurately in the temperature angular spectrum [6]. This corresponds to $\eta \equiv n_b/n_\gamma = (6.6 \pm 0.3) \times 10^{-10}$, where n_b and n_γ are baryon and photon number densities, via the relation $\eta = \omega_b/(3.65 \times 10^7)$. Refs [1, 2, 3, 4] take this well-determined WMAP ω_b as the BBN input[36] and calculate the light elements abundances and their theoretical errors using improved evaluations of nuclear reaction rates and uncertainties. The results are compared with the received measurements of the primordial abundances of three light elements, D (Ref. [7]), ^{4}He (Refs. [8] or [9]) and ^{7}Li (Refs. [10] or [11]). Although there are small differences concerning their adopted reaction rates or observation data, their conclusions agree: from the WMAP baryon density, the predicted abundances are highly con-

sistent with the observed D but not with ^{4}He or ^{7}Li. They are produced more than observed. Especially, the ^{7}Li-WMAP discrepancy is severer and it may require an explanation.

The most conservative and likely interpretation of such discrepancy is that systematic errors in the primordial ^{4}He and ^{7}Li measurements are underestimated in spite of the thorough analysis hitherto. Or, as Ref. [2] has pointed out, it is possible that since the cross section of the reaction ^{7}Be(d,p)2^{4}He has not been measured for the BBN energy range, it could reduce the ^{7}Li yield to match with the observation if the rate turns out to be hundreds times more than the often neglected value obtained by the extrapolation.

If the discrepancy can not be attributed to systematic errors, we would have to invoke new physics to reduce their abundances. Actually, some approaches to reduce ^{7}Li by astrophysical means, such as nonstandard depletion mechanism inside stars, are discussed in Refs. [1, 3, 12] and references therein.

What we seek in this paper is a cosmological solution. For a long time, not a few non-standard models are known to affect ^{4}He abundance but none of them seem to be able to solve the discrepancy. For example, non-standard expansion rate (extra relativistic degrees of freedom) and/or large lepton asymmetry change ^{4}He too much while adjusting ^{7}Li to its observed value [13, 14, 15]. A varying fine structure constant (electromagnetic coupling constant) can relieve the tension between either D and ^{4}He or D and ^{7}Li but not the three elements together [16]. At this time, only bolder attempt such as to combine non-standard expansion rate and a varying fine structure constant investigated by two of the authors in Ref. [17] seems to be able to accommodate D, ^{4}He and ^{7}Li simultaneously, but whether the introduction of these non-standard ingredients can fit the WMAP data is not fully checked yet [37].

In this paper, we investigate a solution which allows different amount of baryons for the BBN and the CMB. Unfortunately this only reconciles the WMAP, D and either ^{4}He or ^{7}Li. We choose to make ^{7}Li consistent with

the observation in this way and consider a large lepton asymmetry in addition in order to accommodate ^{4}He too. One of the advantages of this scenario is that both the additional baryons and lepton asymmetry can be produced from Q-balls, which also generate the original baryons before the BBN.

In next section, we explain the discrepancy briefly and investigate how the prediction of the primordial light element abundances is affected by the additional baryons after the BBN. After we show that is not enough to solve the discrepancy, we introduce the lepton asymmetry and calculate how much extra baryons and lepton asymmetry are needed to be a solution. In section III, we describe how to generate required baryons and leptons. We conclude in section IV.

II.   A SOLUTION TO THE DISCREPANCY

In this section, we show that three elements abundances and the WMAP data are not consistent within the standard framework of cosmology but they are reconciled with the appearance of additional baryons after BBN and the existence of the large lepton asymmetry before the BBN. We also compute how much of those are necessary to be a solution.

A.   The discrepancy among the light elements abundances and WMAP

First of all, we summarize the measured baryon density from the BBN and CMB in the left three panels in Fig 1. We compute the theoretical abundances of ^{4}He, D and ^{7}Li and their uncertainties by Monte Carlo simulations using the values obtained in Ref. [19] based on the reaction rates compiled in Ref. [20]. These are compared with the observations of three light elements. We adopted the following data:

$$Y_{^4\text{He}} = 0.238 \pm 0.002 \pm 0.005, \qquad (1)$$
$$(\text{D/H}) = 2.78^{+0.44}_{-0.38} \times 10^{-5}, \qquad (2)$$
$$(^7\text{Li/H}) = 1.23^{+0.68}_{-0.32} \times 10^{-10} \ (95\%), \qquad (3)$$

where Eq. (1) for ^{4}He mass fraction is taken from Ref. [8] (FO), Eq. (2) for D to H ratio in numbers from Ref. [7], and Eq. (3) for ^{7}Li to H ratio in numbers from Ref. [10] (R). In Eq. (1), the first uncertainty is statistical and the second one is systematic, which are added in quadrature to be the total observational uncertainty. The systematic errors are already included in the error bars of the other two elements. In Eq (3), quoted uncertainty is 95% and we take its half value to be 1σ uncertainty. As indicated by the three boxes in the figure, the ^{4}He and ^{7}Li measurements indicate $\eta \approx (2 \sim 4) \times 10^{-10}$, but much higher value $\eta \approx (6 \sim 7) \times 10^{-10}$ is necessary to explain the D measurement.
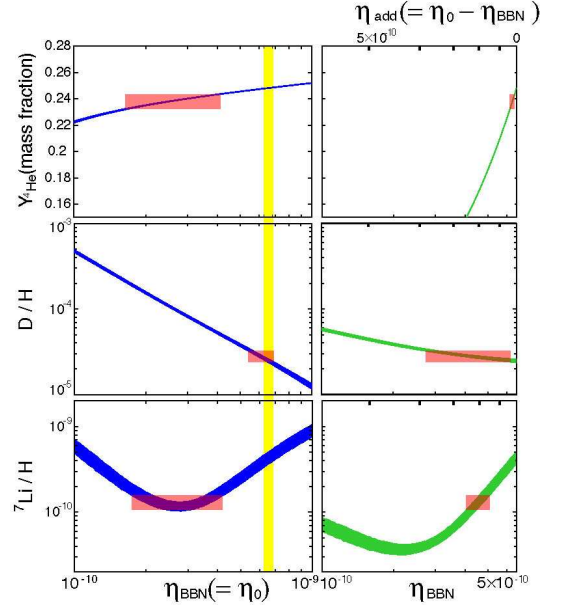

FIG. 1:   In the left column, familiar (namely, η at present, η_0, is same as the one at the BBN, η_{BBN}.) standard BBN calculations of ^{4}He, D and ^{7}Li abundances as functions of η are expressed by three dark-shaded curves whose widths show theoretical 1σ uncertainties. The bar penetrating the figures displays η measured by the WMAP with 1σ uncertainty. In the right column, the light-shaded curves indicate the abundances modified by the baryon appearance after the BBN. In this case, we assume that η is increased from η_{BBN} to be the WMAP measured value, $\eta_0 = \eta_{\text{WMAP}} = 6.6 \times 10^{-10}$. On top of the figures, we mark the scale to tell the amount of added η after the BBN, where $\eta_0 = \eta_{\text{BBN}} + \eta_{\text{add}}$. In both columns, the observational 1σ uncertainties are expressed by the vertical extension of the boxes, which are drawn to overlap the theory curves so that their horizontal extension shows allowed ranges of η.

On superposing the WMAP measured value [38],

$$\eta = (6.6 \pm 0.3) \times 10^{-10}, \qquad (4)$$

the discrepancy seems to be severer. The range of Eq. (4) is expressed by the narrow vertical bar in Fig. 1, overlapping only with the η range deduced from D. The baryon density measured by the WMAP and the one by either ^{4}He or ^{7}Li abundances are not very consistent.

We quantify the discrepancy by calculating χ^2 as a function of η,

$$\chi^2 = \sum_i \frac{(a_i^{th}(\eta) - a_i^{obs})^2}{(\sigma_i^{th})^2 + (\sigma_i^{obs})^2} + \frac{(\eta - \eta_{\text{WMAP}})^2}{\sigma_{\text{WMAP}}^2}, \qquad (5)$$

where a_i and σ_i are respectively abundances and their 1σ uncertainty of the element i. Their theoretical values are calculated from Monte Carlo simulations and observational values are those of Eqs. (1)$\sim$(3). For asymmetric errors, we adopt conservatively the larger one as 1σ error (for ^{7}Li, we divide the error in Eq. (3) by two as

explained above). We use the value of Eq. (4) for the second term. By taking the sum over three elements D, ^{4}He and ^{7}Li, we can investigate overall consistency and by choosing a particular element as i, we can study whether that element is consistent with the WMAP result.

The results are Figs. 2 and 3. Fig. 2 shows the 2 two degree of freedom $\chi^2_{(2)}$ calculated from each element measurement and WMAP. Fig. 3 shows the four degree of freedom $\chi^2_{(4)}$ from three elements measurements and WMAP. As expected from Fig. 1, Fig. 2 shows that D is highly consistent with WMAP but not for ^{4}He and ^{7}Li. When we analyze with the combined data of three elements and WMAP, we see in Fig. 3 that there is no baryon density range to explain the light elements abundances and the CMB. For details, ^{4}He-WMAP discrepancy is not very severe but ^{7}Li is definitely inconsistent with WMAP and this ^{7}Li discrepancy mainly raises the overall χ^2. Therefore, a task worth challenging would be to look for a cosmological model which can adjust ^{7}Li abundance to the observed value while not amplifying the mild ^{4}He-WMAP discrepancy. Of course, it is all the better to alleviate the tension of ^{4}He in addition.

We here comment on the other ^{4}He and ^{7}Li measurements. Ref. [9] (IT) reports $Y_{^4\text{He}} = 0.2421 \pm 0.0021$ and Ref. [11] (B) reports $\log[(^7\text{Li/H})] + 12 = 2.34 \pm 0.056 \pm 0.06$. The systematic effects are already included in the uncertainty in Ref. [9]'s ^{4}He data. For Ref. [11]'s ^{7}Li data, the statistical error and systematic error are added in quadrature so that $[(^7\text{Li/H})] = 2.19^{+0.46}_{-0.38} \times 10^{-10}$. The results using those data instead of Ref. [8]'s ^{4}He and/or Ref. [10]'s ^{7}Li are also shown in Figs. 2 and 3. Ref. [9]'s ^{4}He is less consistent with WMAP than Ref. [8]'s because of much less uncertainty in spite of the higher central value. It is tempting to address a strong ^{4}He-WMAP discrepancy issue on the basis of Ref. [9]'s ^{4}He but we adopt conservative Ref. [8]'s value to focus on ^{7}Li discrepancy problem. For ^{7}Li, we see that the use of Ref. [11]'s value relaxes the discrepancy with WMAP. We adopt Ref. [10]'s measurement because they analyze the observations with lower and broader range of metallicity, but we note that considerable discrepancy still exists for Ref. [11]'s ^{7}Li.

B. Effects of additional baryons after BBN

Roughly speaking, the discrepancy exists because the WMAP data needs more baryons than those required to account for the primordial light elements abundances, especially ^{4}He and ^{7}Li. Then a naive solution would be allowing to increase the baryons after the BBN to the amount required to explain the WMAP data before the physics which form the acoustic peaks takes place.

However, such increase in the baryons (in the form of protons $i.e.$ H nucleus) considerably affects the observation of the light elements abundances because they are always measured in terms of the ratio to H. Since the numerator does not change and the denominator increases,
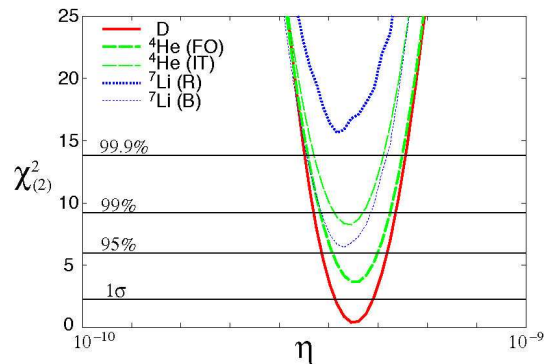

FIG. 2: $\chi^2_{(2)}$ calculated from a single element measurement and WMAP. The different types of lines use the data of D [7] (solid line), ^{4}He of Fields and Olive (FO) [8] (thick dashed line), ^{4}He of Izotov and Thuan (IT) [9] (thin solid line), ^{7}Li of Ryan $et\ al.$ (R) [10] (thick dotted line), and ^{7}Li of Bonifacio $et\ al.$ (B) [11] (thin dotted line). The horizontal lines correspond to, from bottom to top, 1σ, 95%, 99% and 99.9% confidence levels derived from two degree of freedom χ^2.
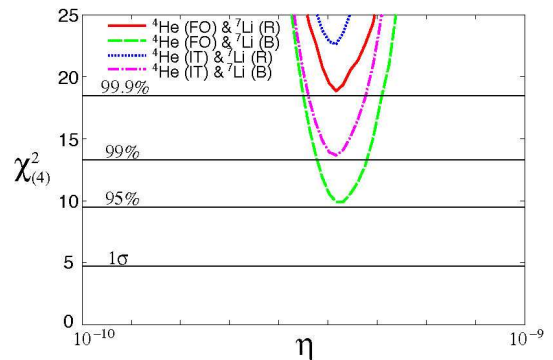

FIG. 3: $\chi^2_{(4)}$ calculated from three elements measurements and WMAP. Expressing each two measurements of ^{4}He and ^{7}Li by the abbreviations introduced in the caption to Fig. 2, the solid line uses FO for ^{4}He and R for ^{7}Li, the dashed line uses FO and B, the dotted line uses IT and R, and the dotted-dashed line uses IT and B. The horizontal lines correspond to, from bottom to top, 1σ, 95%, 99% and 99.9% confidence levels derived from four degree of freedom χ^2.

the abundances decrease in general. To quantify this effect, let η_{BBN} denote the baryon-to-photon ratio during the BBN and let it increase by η_{add} (without entropy production) to be $\eta_{\text{WMAP}} \equiv 6.6 \times 10^{-10}$ after the BBN but well before the matter-radiaion equality. They of course satisfy $\eta_{\text{WMAP}} = \eta_{\text{BBN}} + \eta_{\text{add}}$. For ^{4}He, the effect is very simple because its abundance is conventionally expressed by a mass fraction: $Y_{^4\text{He}} \equiv 4n_{^4\text{He}}/n_b$, where $n_{^4\text{He}}$ is the number density of ^{4}He. Noting that since entropy is not produced, the photon number density scales as a^{-3}, where a is the scale factor, the ^{4}He mass fraction is modified from the value when the BBN ends, $Y_{^4\text{He}}^{(\text{BBN})}$,

to the one we observe, $Y_{^4\text{He}}^{(\text{obs})}$, as

$$Y_{^4\text{He}}^{(\text{obs})} = Y_{^4\text{He}}^{(\text{BBN})} \frac{\eta_{\text{BBN}}}{\eta_{\text{WMAP}}}. \tag{6}$$

For D and ^{7}Li, since the abundance is expressed by the ratio to H in numbers,

$$(\text{D/H})_{obs} \equiv (\text{D/H})_{\text{BBN}} \frac{R_{\text{BBN}}}{R_{\text{BBN}} + \eta_{\text{add}}}, \tag{7}$$

where R_{BBN} denotes the ratio of H to photon in numbers during the BBN,

$$R_{\text{BBN}} \equiv \left[\frac{n_H}{n_\gamma} \right]_{\text{BBN}} = \eta_{\text{BBN}}(1 - Y_{^4\text{He}}^{(\text{BBN})}). \tag{8}$$

In Eq. (8), we regard abundances of the light elements other than H and ^{4}He are negligibly small.

Using the Eqs. (6), (7) and (8), we can predict the observed abundances modified by the baryon appearance after the BBN as shown in the right three panels in Fig 1. Since we only consider the increase in η, they are truncated at η_{WMAP} and η_{add} increases to the left. Compared with the standard case in the panels on the left hand side, the abundances become smaller for greater η_{add} as expected and it is conspicuous for ^{4}He.

Similar to the standard BBN case, the comparison with the observations is made by three boxes in the figure. We see D and either ^{4}He or ^{7}Li can be reconciled with appropriate additional baryons but not for three elements together.

To obtain a solution to reconcile three elements abundance measurements simultaneously, we first choose to make D and ^{7}Li consistent by the adding baryons $\eta_{\text{add}} \approx 1.5 \times 10^{-10}$. Then we introduce a (negative) lepton asymmetry before the onset of the BBN in order to enhance ^{4}He abundance (about 1.5 times) while retaining D and ^{7}Li abundances. We next quantify how much lepton asymmetry is needed.

C. Plus a lepton asymmetry before BBN

The lepton asymmetry is parametrized by the degeneracy parameter $\xi_e \equiv \mu_e/T$ where μ_e is the electron-type neutrino chemical potential. Taking into account the tendency toward flavor equilibration [21], we assume every flavor has the same amount of asymmetry for concreteness.

Since we only consider $|\xi_e| \lesssim O(1)$, its contribution as the extra relativistic degree of freedom is very small and the effect on the nuclear beta equilibrium, $p + e^- \leftrightarrow n + \nu_e$ dominates. This property is important because it ensures that the baryon density measurement by CMB as Eq. (4) is not disrupted. When there is a negative lepton asymmetry ($\xi_e < 0$), neutrinos are less than anti-neutrino and the equilibrium shifts to increase n relative to p. This is
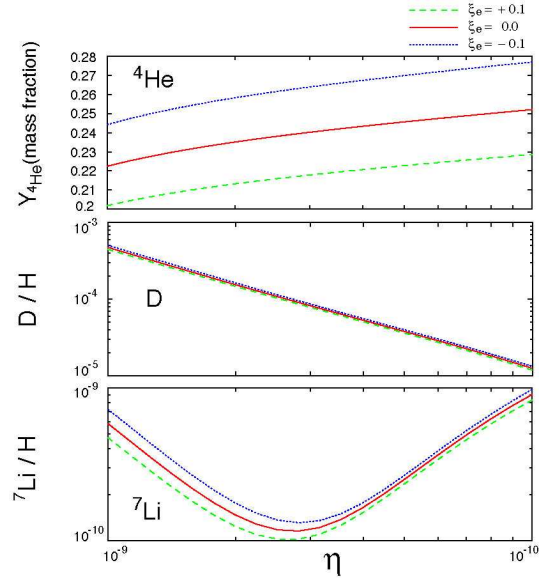

FIG. 4: ξ_e-dependence of light element abundances. The cases for $\xi_e = 0$, $+0.1$, -0.1 are drawn with solid, dashed, and dotted lines.

formulated as the following equation. Since their number densities obey Boltzmann statistics, an equilibrium number ratio at temperature T is [22]

$$\frac{n_n}{n_p} = \exp\left[-\frac{\Delta m}{T} - \xi_e \right], \tag{9}$$

where Δm is the neutrino-proton mass difference and $\Delta m \approx 1.29$MeV. From this expression it is easy to see ^{4}He is sensitive to non-zero ξ_e because its abundance is approximately written as

$$Y_{^4\text{He}} = \left. \frac{2n_n}{n_n + n_p} \right|_f = \frac{2}{1 + (n_p/n_n)_f} = \frac{2}{1 + e^{\Delta m/T_f + \xi_e}} \tag{10}$$

where the subscript f means the values at the weak interaction freeze-out and $T_f \approx 0.7$MeV, showing ^{4}He mass fraction depends exponentially on ξ_e. This is illustrated in the top panel of Fig. 4. The dependences of D and ^{7}Li on ξ_e are also shown but they are very small. This is important because we do not want to spoil the consistency between D and ^{7}Li by the introduction of the lepton asymmetry.

From Eq. (10), we estimate $\xi_e \sim -0.3$ is necessary in order to make the ^{4}He abundance larger and achieve the scenario mentioned at the end of the previous subsection. To confirm such an estimation, we search for the allowed parameter region on η_{add}-ξ_e plane by calculating χ^2 as a function of those two parameters. Since we fix the baryon density after BBN at the WMAP central value, the χ^2 here is calculated using three light elements data as Eq. (5) with the last term omitted. The inclusion of the small uncertainty in WMAP baryon density would make the allowed region just a little larger. The
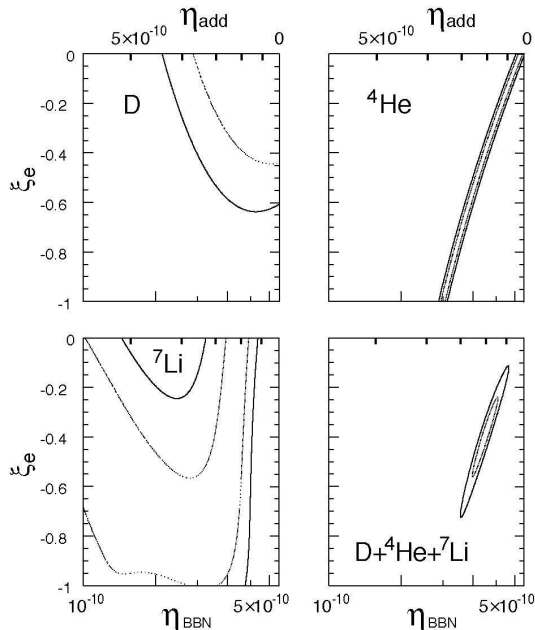
FIG. 5: 1σ (dotted lines) and 95% (solid lines) confidence levels in the $\eta - \xi_e$ plane determined by each light elements observations alone and by three elements combined.

results are displayed in Fig. 5. The allowed regions determined from each element are understood from Figs. 1 and 4, and their product set makes the region shown in the bottom-right panel, which accommodates three elements. Especially, there is no solution for $\xi_e = 0$ or $\eta_{\rm add} = 0$, and the best solution is located at about $(\eta_{\rm add}, \xi_e) = (2 \times 10^{-10}, -0.4)$, as expected during the argument thus far.

III. Q-BALL BARYO- AND LEPTOGENESIS

In this section, we show a model that explains the large lepton asymmetry, the initial baryon asymmetry before BBN, and additional baryon appearance after the BBN all together. To accomplish this let us consider the Affleck-Dine (AD) mechanism [23] and the subsequent Q-ball formation [24, 25, 26] in the gauge-mediated supersymmetry (SUSY) breaking model. Before turning to a close examination of the model, it will be useful to summarize our basic strategy. The mechanism generating large lepton asymmetry we adopt here is based on Ref. [27]. The AD mechanism can produce large (and negative) lepton asymmetry by choosing an appropriate leptonic flat direction such as $e_2 L_1 L_3$, where the subindices represent the generation. After the flat direction starts oscillating, the AD field experiences the spatial instability and deforms into nontopological solitons, Q-balls (L-balls). Then, almost all the produced lepton numbers are absorbed into the L-balls [26, 28]. If the lifetime of such L-balls is longer than the on-

set of electroweak phase transition but shorter than the epoch of BBN, the large lepton asymmetry is protected from sphaleron effects [29] and later released into the universe by the decay of the L-balls. On the other hand, small (negative) lepton numbers are evaporated from the L-balls due to thermal effects before the electroweak phase transition, which are transformed into small baryon asymmetry through the sphaleron effect. Thus generated baryon number is the source for light element synthesis. Additional baryon number after the BBN can also be explained by the use of Q-balls. If the dimension of a flat direction is not so large, other flat directions can obtain nonzero vevs simultaneously. For instance, udd direction is compatible with eLL direction. The baryon asymmetry generated by the udd direction is also absorbed into Q-balls (B-balls). If the B-balls decay after the relevant BBN epoch, they can explain the late-time baryon appearance. In order to avoid dissociating the synthesized light elements with the decay products, the mass per unit baryon charge of the B-ball must be tacitly chosen to be slightly above the neutron or proton mass. To this end, we take $m_{3/2} = 1\,{\rm GeV}$ in the following discussion (see Eq. (18)). It should be noted that the AD mechanism and associated Q-ball formation can account for both the large lepton asymmetry and the baryon asymmetry before and after the BBN.

A. Affleck-Dine Mechanism and Q-balls

First off, let us review the AD mechanism and several properties of Q-balls. In the minimal supersymmetric standard model (MSSM) there exist flat directions, along which there are no classical potentials in the supersymmetric limit. Since flat directions consist of squarks and/or sleptons, they carry baryon and/or lepton numbers, and can be identified as the Affleck-Dine (AD) field. For a definite discussion, we adopt eLL and udd directions as the AD fields. It is of use to parametrize the flat direction with a single complex scalar field Φ, so we express eLL and udd directions as Φ_L and Φ_B, respectively.

The flat directions are lifted by supersymmetry breaking effects. In the gauge-mediated SUSY breaking model, the potential of a flat direction is parabolic at the origin, and almost flat beyond the messenger scale [24, 28, 30],

$$V_{gauge} \sim \begin{cases} m_\phi^2 |\Phi|^2 & (|\Phi| \ll M_S), \\ M_F^4 \left(\log \dfrac{|\Phi|^2}{M_S^2} \right)^2 & (|\Phi| \gg M_S), \end{cases} \quad (11)$$

where m_ϕ is a soft breaking mass $\sim O(1{\rm TeV})$, M_F is the SUSY breaking scale, and M_S is the messenger mass scale.

Since gravity always exists, flat directions are also lifted by gravity-mediated SUSY breaking effects [31],

$$V_{grav} \simeq m_{3/2}^2 \left[1 + K \log \left(\frac{|\Phi|^2}{M_*^2} \right) \right] |\Phi|^2, \quad (12)$$

where K is the numerical coefficient of the one-loop corrections and M_* is the gravitational scale ($\simeq 2.4 \times 10^{18}$ GeV). This term can be dominant only at high energy scales because of small gravitino mass $\sim O(1 \text{ GeV})$.

The non-renormalizable terms, if allowed by the symmetries of Lagrangian, can exist and lift the flat directions;

$$V_{NR} = \frac{|\Phi|^{2n-2}}{M^{2n-6}}, \tag{13}$$

where M is a cut off scale of the non-renormalizable term. In our scenario described in the next subsection, Φ_B is lifted by the non-renormalizable potential, while Φ_L feels only the SUSY breaking potentials.

The baryon and lepton number is usually created just after the AD field starts coherent rotation in the potential, and its number density $n_{B,L}$ is estimated as

$$n_{B,L}(t_{osc}) \simeq \varepsilon \omega \phi_{osc}^2, \tag{14}$$

where $\varepsilon(\lesssim 1)$ is the ellipticity parameter, which represents the strongness of the A term, and ω and ϕ_{osc} are the angular velocity and amplitude of the AD field at the beginning of the oscillation (rotation) in its effective potential.

Actually, however, the AD field experiences spatial instabilities during its coherent oscillation, and deforms into nontopological solitons called Q-balls [24, 25, 26]. When the zero-temperature potential V_{gauge} dominates at the onset of coherent oscillation of the AD field, the gauge-mediation type Q-balls are formed. Their mass M_Q and size R_Q are given by [32]

$$M_Q \sim M_F Q^{3/4}, \qquad R_Q \sim M_F^{-1} Q^{1/4}. \tag{15}$$

From the numerical simulations [26, 28], the produced Q-balls absorb almost all the charges carried by the AD field and the typical charge is estimated as [28]

$$Q \simeq \beta \left(\frac{\phi_{osc}}{M_F} \right)^4 \tag{16}$$

with $\beta \approx 6 \times 10^{-4}$.

There are also other cases where V_{grav} dominates the potential at the onset of coherent oscillation of the AD field. If K is positive, Q-balls do not form until the AD field leaves the V_{grav} dominant region. Later it enters the V_{gauge} dominant region and experiences instabilities so that the gauge-mediation type Q-balls are produced (delayed-type Q-balls) [28]. The charge of the delayed-type Q-ball is

$$Q \sim \beta \left(\frac{\phi_{eq}}{M_F} \right)^4 \sim \beta \left(\frac{M_F}{m_{3/2}} \right)^4 \tag{17}$$

with $\phi_{eq} \sim M_F^2/m_{3/2}$. Here the subscript "eq" denotes a value when the gauge- and the gravity-mediation potentials become equal. Thus the delayed-type Q-balls are formed at $H_{eq} \sim M_F^2/M_*$.

On the other hand, if the coefficient of the one-loop correction K is negative, the gravity-mediation type Q-balls ("new" type) are produced [33]. The typical value of their mass, size, and charge are estimated as

$$M_Q \sim m_{3/2}Q, \qquad R_Q \sim (\sqrt{|K|}m_{3/2})^{-1},$$
$$Q \sim \bar{\beta} \left(\frac{\phi_{osc}}{m_{3/2}} \right)^2 \tag{18}$$

with $\bar{\beta} = 6.0 \times 10^{-3}$.

Finally let us mention the decay of Q-balls. In the case of L-balls, they decay into leptons such as neutrinos via wino exchanges. Also B-balls can decay into nucleons such as protons and neutrons via gluino exchanges. The decay rate of Q-balls is bounded as [34]

$$\left| \frac{dQ}{dt} \right| \lesssim \frac{\omega^3 A}{192\pi^2}, \tag{19}$$

where A is a surface area of the Q-ball. For L-balls, the decay rate is estimated as a value of the order of the upper limit, while it must be somewhat suppressed for B-balls, if the mass per unit baryon number, M_Q/Q, is close to the nucleon mass $\sim 1\text{GeV}$.

B. B- and L-balls

Now we detail the scenario. In order to generate $O(1)$ lepton asymmetry, the AD field responsible for large lepton asymmetry should start to oscillate from the gravitational scale, i.e., $\phi_{L,osc} = M_*$, which leads to the formation of delayed-type L-balls. Meanwhile the value of ϕ_B at the onset of the oscillation must be suppressed due to the existence of the non-renormalizable term. Also ϕ_B is assumed to form new type B-balls, which decay after the BBN. Let us see if this setup can be naturally realized step by step.

First of all, of the two flat directions, only ϕ_B should be lifted by the non-renormalizable term, which can be explained by the R-symmetery. For instance, assigning R-charges $\frac{2}{3}$ to e, L, H_u, and H_d, $\frac{1}{3}$ to u and d, and 1 to Q, non-renormalizable terms for eLL are forbidden, while the following superpotential can lift the udd direction;

$$W_{NR}^{(udd)} = \frac{9(udd)^2}{2M^3} = \frac{\Phi_B^6}{6M^3},$$
$$V_{NR}^{(udd)} = \frac{|\Phi_B|^{10}}{M^6}. \tag{20}$$

During inflation, ϕ_B thus sits at the minimum $\sim (HM^3)^{1/4}$ determined by balancing the non-renormalizable term and the negative Hubble-induced mass term.

Second, the abundance of the late-time baryon appearance must be of the order of $\eta_{\text{add}} \sim O(10^{-10})$. According to the result of Ref. [27], both the large lepton asymmery, $|\xi_e| \sim O(0.1)$, and the baryon asymmetry necessary for the BBN, $\eta_{\text{BBN}} \sim O(10^{-10})$, can be successfully

generated.[39] Therefore it is enough to estimate the relative abundance of the additional baryon number to the lepton asymmetry. Using Eq. (14), the baryon number of the *udd* direction is suppressed by $(\phi_B/\phi_L)^2$, which is calculated as

$$\left(\frac{\phi_B}{\phi_L}\right)^2 \sim \left(\frac{(m_{3/2}M^3)^{1/4}}{M_*}\right)^2 \sim 10^{-9}, \qquad (21)$$

where we assumed $M \sim M_*$ and $m_{3/2} \sim 1\text{GeV}$. Thus we can naturally obtain the desired abundance, $\eta_{\text{add}} \sim O(10^{-10})$.

Thirdly, the sign of K should be positive for Φ_L, while negative for Φ_B. Unless the flat direction includes the third generation superfields, the sign of K tends to be negative due to the contribution from the gauge interactions. This is because the contribution to K from Yukawa (gauge) interactions is positive (negative). Note that the Yukawa coupling not only for top but also for bottom and tau particles can be $O(1)$ for large $\tan\beta$. Therefore, if we choose the flat directions as *e.g.*, $e_2L_1L_3$ and $u_1d_2d_1$, the sign of K for the two directions is the desired one.

Lastly, we need to show that the new type B-balls decay after the relevant BBN epoch. The decay rate of the B-ball is

$$\Gamma_Q \equiv \frac{1}{Q}\left|\frac{dQ}{dt}\right| = \frac{m_{3/2}^{5/2}}{48\pi\bar\beta|K|M^{3/2}}, \qquad (22)$$

where we used Eq. (19). Simply equating this quantity with the Hubble parameter, we have the relatively high decay temperature,

$$T_d \simeq 0.08\,\text{MeV}\left(\frac{|K|}{0.1}\right)^{1/2}\left(\frac{m_{3/2}}{1\text{GeV}}\right)^{5/4}\left(\frac{M}{M_*}\right)^{-3/4}, \qquad (23)$$

around which the light elements are being synthesized. However, as noted above, the decay rate is suppressed if the mass per unit baryon charge is very close to the nucleon mass, leading to smaller decay temperature. There-fore we expect the new type B-balls decay after the light element synthesis ceases to proceed.

To sum up the major characteristics of our scenario, the Q-balls protect not only lepton asymmetry from the sphaleron effects, but also baryon asymmetry from the BBN processes, which leads to the late-time baryon appearance.

IV. CONCLUSION

Concerning recent cosmological observations, there seems to be conflicting measurements of the baryons in the universe, namely, the baryon density deduced from the CMB observation by the WMAP or the primordial D abundance is much higher than the one derived from ^{4}He or ^{7}Li abundances. In this paper, we have proposed a scenario to reconcile such inconsistency by adding baryons after the BBN and assuming a lepton asymmetry before the BBN. The introduction of the additional baryons leads to success in explaining the observed low abundance of ^{7}Li without recourse to special models of stellar depletion. Also it was shown that the scenario can be naturally implemented in the AD mechanism, where Q-balls play an essential role in preserving extra lepton and baryon asymmetries. We should note that this is the first cosmological scenario that can completely remove the long-standing tension among the three light elements and CMB. According to our result, amazingly, about one third of the baryon we observe in the present universe might have been "sterile" during the BBN epoch. Such illuminating history of the universe might be confirmed through further observational results with better accuracy in the future.

ACKNOWLEDGEMENTS

[1] R. H. Cyburt, B. D. Fields and K. A. Olive, Phys. Lett. B **567**, 227 (2003) [arXiv:astro-ph/0302431].

[2] A. Coc, E. Vangioni-Flam, P. Descouvemont, A. Adahchour and C. Angulo, Astrophys. J. **600**, 544 (2004) [arXiv:astro-ph/0309480].

[3] A. Coc, E. Vangioni-Flam, P. Descouvemont, A. Adahchour and C. Angulo, arXiv:astro-ph/0401008.

[4] R. H. Cyburt, arXiv:astro-ph/0401091.

[5] D. N. Spergel *et al.*, Astrophys. J. Suppl. **148**, 175 (2003) [arXiv:astro-ph/0302209].

[6] L. Page *et al.*, Astrophys. J. Suppl. **148**, 233 (2003) arXiv:astro-ph/0302214.

[7] D. Kirkman, D. Tytler, N. Suzuki, J. M. O'Meara and D. Lubin, Astrophys. J., Suppl. Ser. **149**, 1 (2003) [arXiv:astro-ph/0302006].

[8] B. D. Fields and K. A. Olive, Astrophys. J. **506**, 177 (1998).

[9] Y. I. Izotov and T. X. Thuan, Astrophys. J. **602**, 200 (2004) [arXiv:astro-ph/0310421].

[10] S. G. Ryan, T. C. Beers, K. A. Olive, B. D. Fields, and J. E. Norris, Astrophys. J. Lett., **530**, L57 (2000).

[11] P. Bonifacio *et al.*, Astron. Astrophys. **390**, 91 (2002) [arXiv:astro-ph/0204332].

[12] D. Romano, M. Tosi, F. Matteucci and C. Chiappini, Mon. Not. Roy. Astron. Soc. **346**, 295 (2003) [arXiv:astro-ph/0308181].

[13] V. Barger, J. P. Kneller, H. S. Lee, D. Marfatia and G. Steigman, Phys. Lett. B **566**, 8 (2003) [arXiv:hep-ph/0305075].

[14] V. Barger, J. P. Kneller, P. Langacker, D. Marfa-

tia and G. Steigman, Phys. Lett. B **569**, 123 (2003) [arXiv:hep-ph/0306061].

[15] G. Steigman, arXiv:hep-ph/0309347.

[16] K. M. Nollett and R. E. Lopez, Phys. Rev. D **66**, 063507 (2002) [arXiv:astro-ph/0204325].

[17] K. Ichikawa and M. Kawasaki, arXiv:hep-ph/0401231.

[18] V. F. Dmitriev, V. V. Flambaum and J. K. Webb, Phys. Rev. D **69**, 063506 (2004) [arXiv:astro-ph/0310892].

[19] R. H. Cyburt, B. D. Fields and K. A. Olive, New Astron. **6**, 215 (2001) [arXiv:astro-ph/0102179].

[20] C. Angulo *et al.*, Nucl. Phys. A **656**, 3 (1999).

[21] A. D. Dolgov, S. H. Hansen, S. Pastor, S. T. Petcov, G. G. Raffelt and D. V. Semikoz, Nucl. Phys. B **632**, 363 (2002) [arXiv:hep-ph/0201287].

[22] E. W. Kolb and M. S. Turner, *The Early Universe* (Addison Wesley, Reading, MA, 1990).

[23] I. Affleck and M. Dine, Nucl. Phys. B **249**, 361 (1985); M. Dine, L. Randall and S. Thomas, Nucl. Phys. B **458**, 291 (1996) [arXiv:hep-ph/9507453].

[24] A. Kusenko and M. E. Shaposhnikov, Phys. Lett. B **418**, 46 (1998) [arXiv:hep-ph/9709492].

[25] K. Enqvist and J. McDonald, Nucl. Phys. B **538**, 321 (1999) [arXiv:hep-ph/9803380].

[26] S. Kasuya and M. Kawasaki, Phys. Rev. D **61**, 041301 (2000) [arXiv:hep-ph/9909509].

[27] M. Kawasaki, F. Takahashi and M. Yamaguchi, Phys. Rev. D **66**, 043516 (2002) [arXiv:hep-ph/0205101].

[28] S. Kasuya and M. Kawasaki, Phys. Rev. D **64**, 123515 (2001) [arXiv:hep-ph/0106119].

[29] V. A. Kuzmin, V. A. Rubakov and M. E. Shaposhnikov, Phys. Lett. B **155**, 36 (1985); S. Y. Khlebnikov and M. E. Shaposhnikov, Nucl. Phys. B **308**, 885 (1988); J. A. Harvey and M. S. Turner, Phys. Rev. D **42**, 3344 (1990).

[30] A. de Gouvea, T. Moroi and H. Murayama, Phys. Rev. D **56**, 1281 (1997) [arXiv:hep-ph/9701244].

[31] K. Enqvist and J. McDonald, Phys. Lett. B **425**, 309 (1998) [arXiv:hep-ph/9711514].

[32] G. R. Dvali, A. Kusenko and M. E. Shaposhnikov, Phys. Lett. B **417**, 99 (1998) [arXiv:hep-ph/9707423].

[33] S. Kasuya and M. Kawasaki, Phys. Rev. Lett. **85**, 2677 (2000) [arXiv:hep-ph/0006128].

[34] A. G. Cohen, S. R. Coleman, H. Georgi and A. Manohar, Nucl. Phys. B **272**, 301 (1986).

[35] A. D. Dolgov and F. Takahashi, Nucl. Phys. B **688**, 189 (2004) [arXiv:hep-ph/0402066].

[36] To be more precise, they adopt $\eta = (6.14 \pm 0.25) \times 10^{-10}$ which is obtained from the running spectral index model value $\omega_b = 0.0224 \pm 0.0009$ via the ω_b-η relation. Since this value is inferred from the combination of CMB, galaxy and Lyman α forest data, we adopt the value quoted in the text which is inferred using only the WMAP data.

[37] A varying deutron binding energy may have the capacity to render internal agreement between the light element abundances and with WMAP [18].

[38] The WMAP group quotes $\eta = \left(6.5^{+0.4}_{-0.3}\right) \times 10^{-10}$ as mean and 68% confidence range [5]. Although our adopted values are slightly different since we derive them from ω_b as explained in Sec. I, the difference scarcely affect our results.

[39] To obtain positive baryon asymmetry, the total lepton asymmetry must be negative. The aim of Ref. [27] was to produce "positive" lepton asymmetry of electron type, with the total lepton asymmetry being negative. Here what we want is $\xi_e \sim O(-0.1) < 0$, therefore the flavor equilibration due to neutrino oscillation [21] does not spoil our scenario. However, for recent work of suppressing such flavor equilibration, see Ref. [35].